Electronic Supplementary Material (ESI) for Physical Chemistry Chemical Physics.

Supplementary Information

Incorporation Efficiency and Inhibition Mechanism of 2'-Substituted Nucleotide Analogs against SARS-CoV-2 RNA-dependent RNA polymerase

Congmin Yuan[1,2], Eshani C. Goonetilleke[1,2], Ilona Christy Unarta[1,2], Xuhui Huang[1,2,*]

[1]*Department of Chemistry, Centre of Systems Biology and Human Health, State Key Laboratory of Molecular Neuroscience, The Hong Kong University of Science and Technology, Kowloon, Hong Kong*

[2]*Hong Kong Center for Neurodegenerative Diseases, Hong Kong Science Park, Hong Kong*

* To whom correspondence may be addressed. Email: xuhuihuang@ust.hk (X. H.)

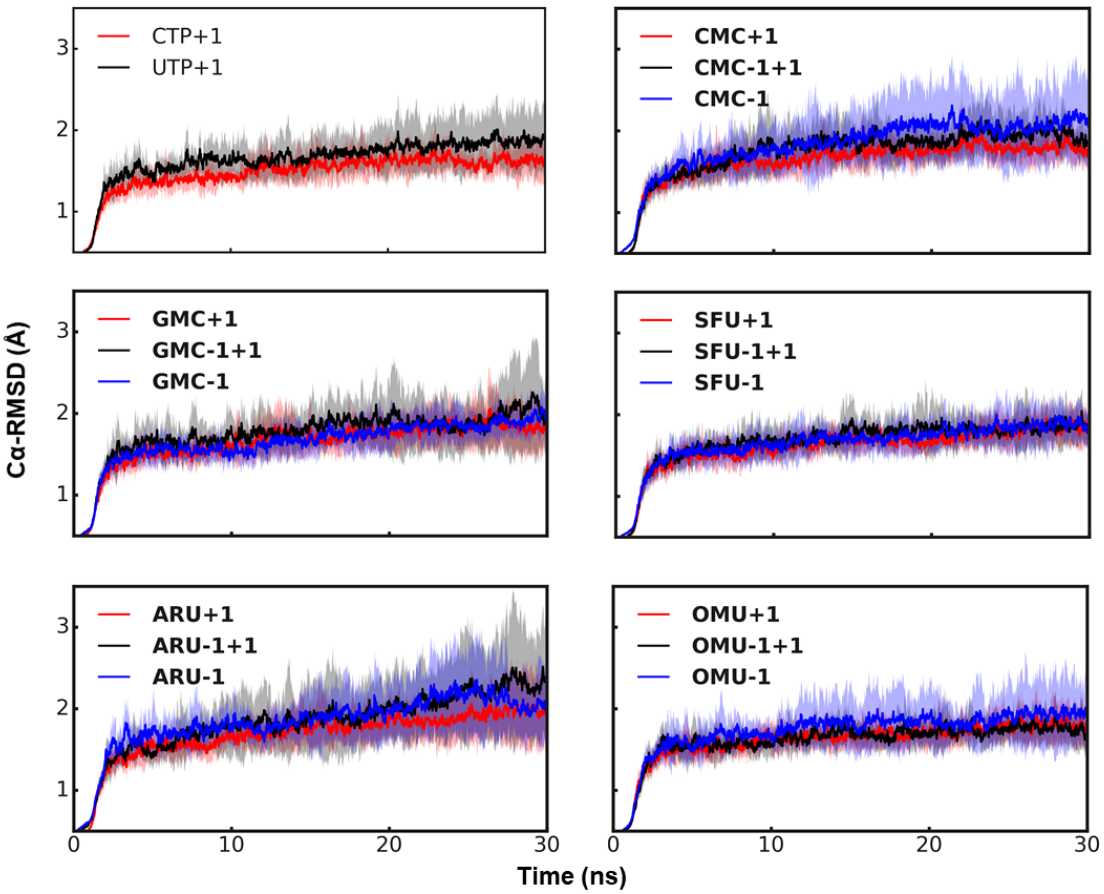

Figure S1. RMSD values of Cα atoms as a function of time in the production run. Cα atoms of the complex including protein, RNA, and nucleotides were used for superposition to the initial and deviation calculation. The mean value over 10 independent trajectories is shown as a solid line, and the shaded regions denote standard deviation.

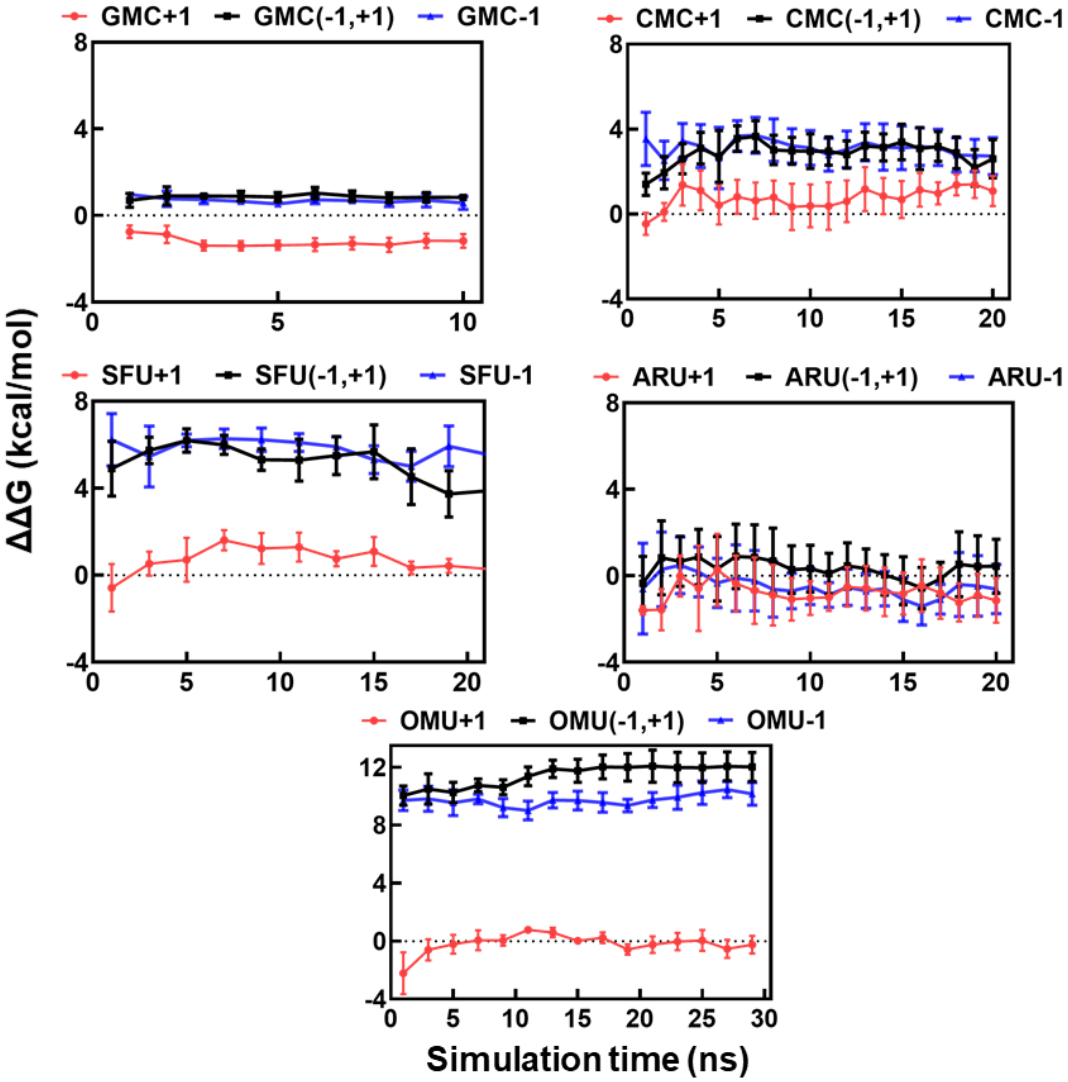

Figure S2. Convergence of the free energy calculations. The $\Delta\Delta G_{binding}$ value changes as a function of transition time in the FEP calculation. The average value is shown as a solid line. The error bar was derived from three independent calculations for each system.

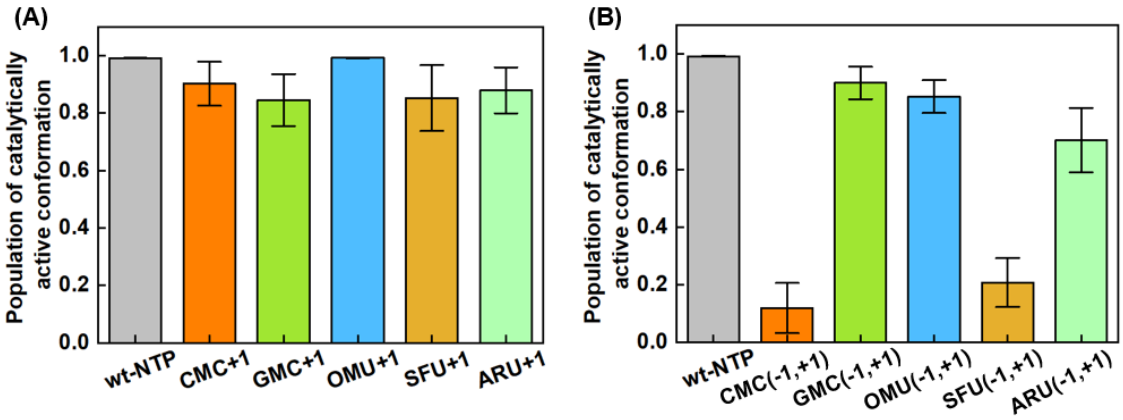

Figure S3. The population of catalytically active conformation in (A) +1 systems and (B) the (-1, +1) systems. O3'-Pα distance smaller than 4 Å was used as the criterion of the catalytically active conformation. An average between CTP+1 and UTP+1 systems was used to represent the wt-NTP system.

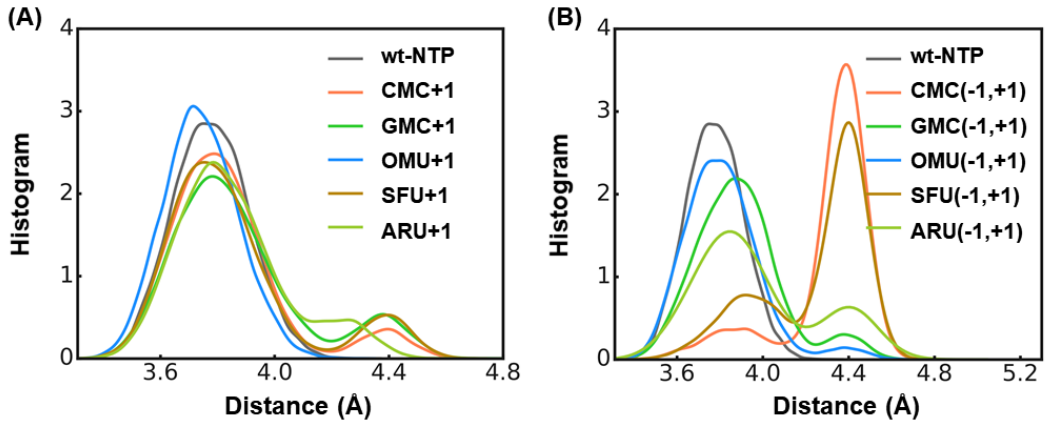

Figure S4. Distribution of distance between MgA and MgB during the MD simulation in (A) +1 systems and (B) the (-1, +1) systems.

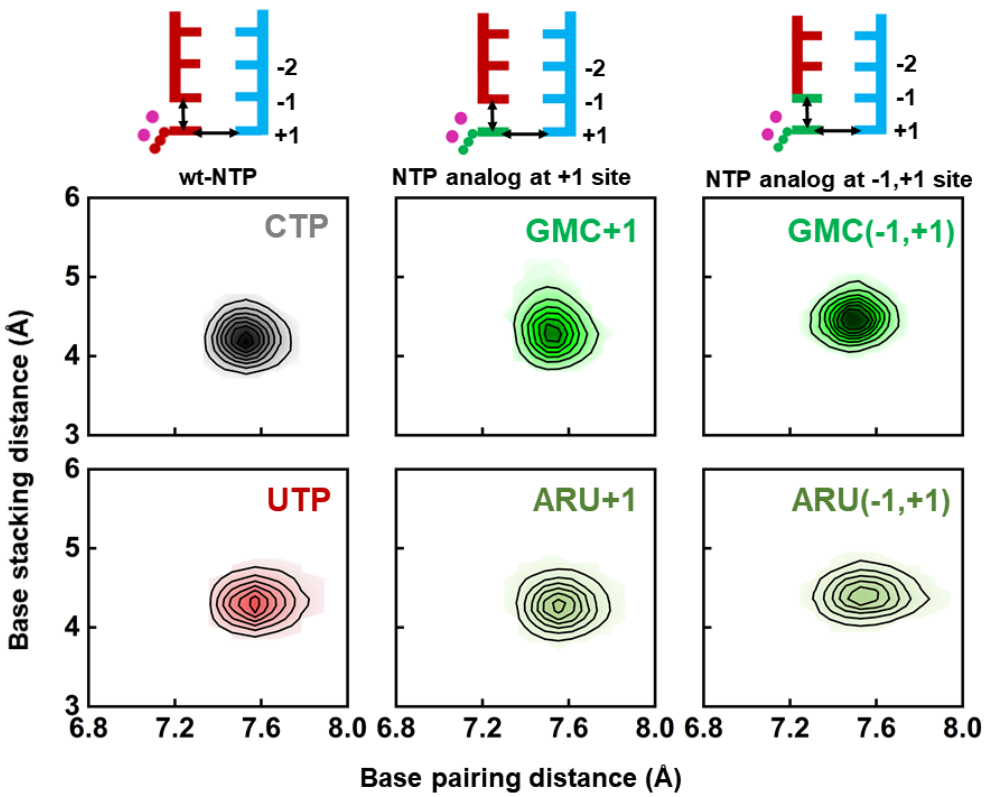

Figure S5. Cartoons in the top panel indicate the NTP at the active site and pairing/stacking nucleotides measured in different systems. Density figures show the distribution of base pairing and base stacking distance between NTP and nucleotides in wild-type and GMC+1, GMC(-1,+1), ARU+1, and ARU(-1,+1) systems.

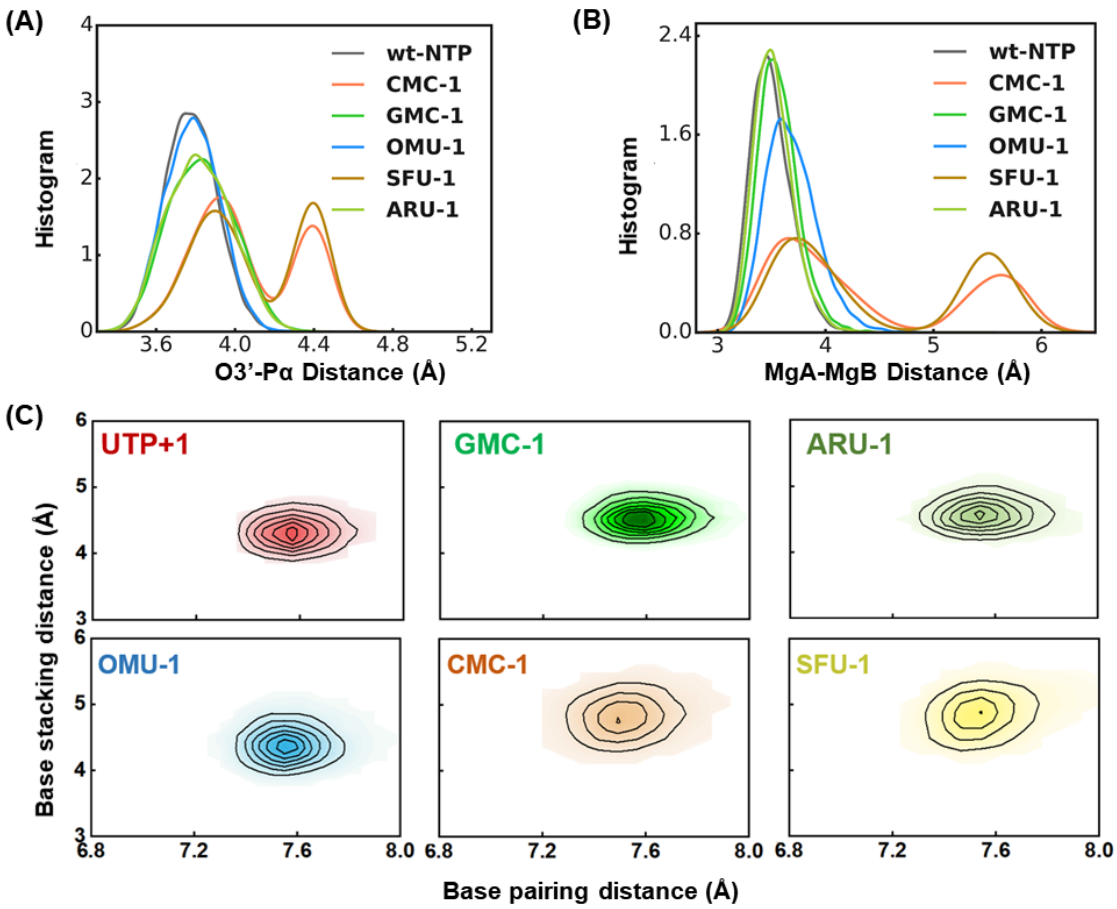

Figure S6. MD simulation results for -1 systems. (A) A plot showing the O3'- Pα distance distribution in -1 systems with nucleotide analogs bound at the -1 sites and wt-NTP at the +1 site. (B) Distribution of the distance between MgA and MgB during the MD simulation for -1 systems. (C) Density figures showing the distribution of base pairing and base stacking distance between NTP and nucleotides in UTP+1 and -1 systems.

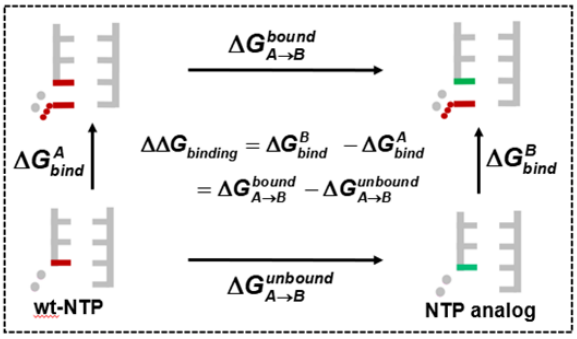

Table S1. Calculated $\Delta\Delta G_{binding}$ for -1 systems

Systems	$\Delta\Delta G_{binding}$ (kcal/mol)	Reference
CMC-1	2.730 ± 0.160	CTP
GMC-1	0.580 ± 0.068	CTP
OMU-1	10.898 ± 0.111	UTP
SFU-1	3.830 ± 0.088	UTP
ARU-1	-0.617 ± 0.141	UTP

Figure S7. Thermodynamical cycle for perturbing NTP from the wild-type to analogs at the -1 site is shown in the panel on the left. The calculated relative binding free energy for the wt-NTP binding to the RdRp active site when the nucleotide analog is already incorporated at the -1 site is shown in table S1 on the right.

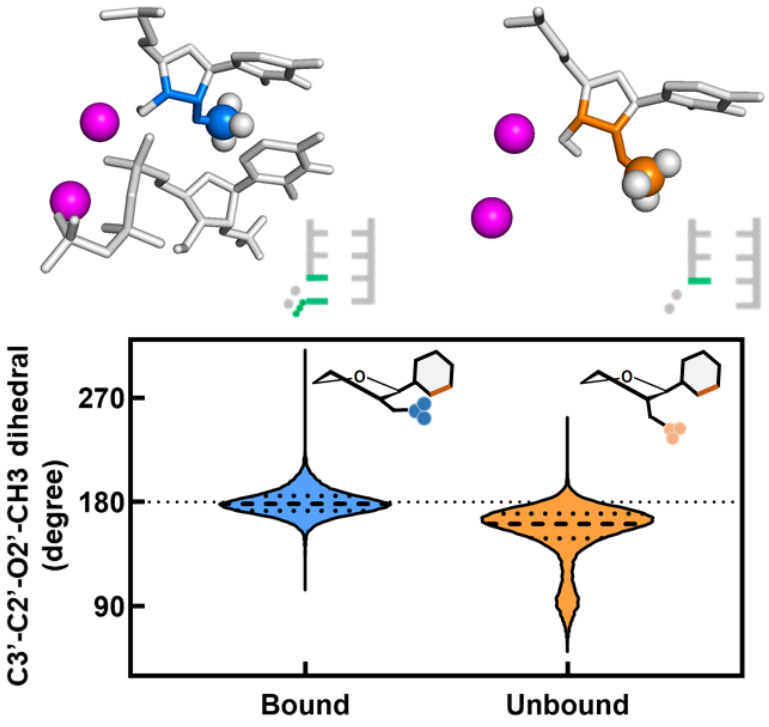

Figure S8. C3'-C2'-O2'-CH3 dihedral distribution of OMU molecules in the end state simulations during FEP calculation. OMU at the -1 site in a bound system and unbound system is shown in blue and orange, respectively.

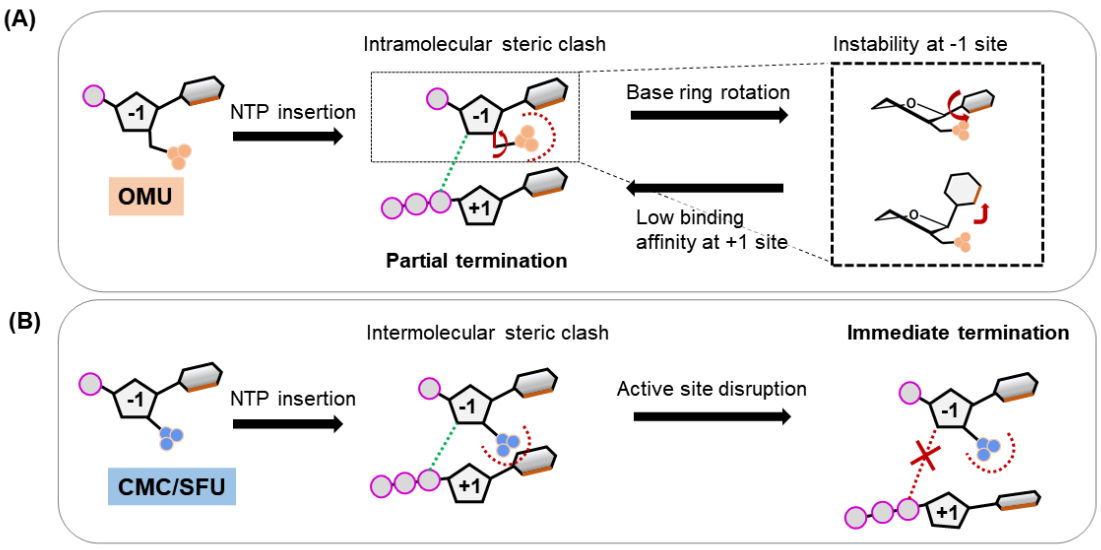

Figure S9. A schematic diagram showing the inhibition mechanism of OMU (A) and CMC/SFU (B).

Table S2. Hydrogen bonding occurrence with NTP analogs at the +1 site

+1 systems	+1 Hbond	Occurrence(%)
CTP+1	2.968±0.003	98.9
CMC+1	2.935±0.017	97.8
GMC+1	2.963±0.006	98.8
UTP+1	1.871±0.020	93.6
OMU+1	1.815±0.014	90.8
SFU+1	1.865±0.019	93.2
ARU+1	1.908±0.007	95.4

Table S3. Hydrogen bonding occurrence with NTP analogs bound at the +1 site and -1 site

(-1,+1) systems	+1 Hbond	Occurrence(%)	-1 Hbond	Occurrence(%)
CMC(-1,+1)	2.926±0.007	97.5	2.893±0.024	96.4
GMC(-1,+1)	2.961±0.005	98.7	2.887±0.012	96.2
OMU(-1,+1)	1.868±0.027	93.4	1.060±0.224	53.0
SFU(-1,+1)	1.763±0.026	88.2	1.870±0.016	93.5
ARU(-1,+1)	1.835±0.011	91.8	1.922±0.016	96.1